Modeling Discontinuities in Dielectric-Loaded Waveguides

KAWTHAR A. ZAKI, SENIOR MEMBER, IEEE, SENG-WOON CHEN, STUDENT MEMBER, IEEE, AND CHUNMING CHEN, STUDENT MEMBER, IEEE

Abstract—**The mode-matching technique is applied to model step discontinuities in dielectric-loaded cylindrical waveguide excited by hybrid modes. It is shown that the solution for the fields obtained by mode matching does not converge unless complex modes are included in the field expansion. If the structure parameters and operating frequency allow for the existence of complex modes, then the purely propagating and evanescent mode fields do not form a complete set, unless complemented by the complex mode fields. Numerical results are presented that clearly illustrate the role of the complex mode fields in the modeling of step discontinuities. Examples are included illustrating the representation of the step discontinuities by a multiport scattering matrix.**

I. INTRODUCTION

IT HAS BEEN shown [1]–[3] that inhomogeneously filled waveguides can support, in addition to the evanescent and the propagating modes, complex modes, characterized by complex propagation constants. Recently, a generalized rigorous analysis of lossless inhomogeneously filled waveguides [4] and numerical methods for the investigation of their properties [5] have been presented, which derived many important properties of complex modes. Generally, numerical search for the propagation constants of complex modes is a much more difficult problem than for the normal propagating and evanescent modes. Complex modes usually exist for very limited ranges of structure parameters and frequency. When solving for discontinuity problems in guiding structures which could support complex modes one is always faced with the problem of whether it is necessary to consider and include complex modes in the solution. This question has recently been addressed for the problem of finline discontinuities [6], where it was shown that ignoring a complex mode results in violation of complex power conservation across the discontinuity.

This paper analyzes the step discontinuity problem in a dielectric-loaded waveguide, together with the role of complex modes in the solution of such a problem. The general structure under consideration is shown in Fig. 1(a). It consists of two semi-infinite dielectric-loaded cylindrical waveguides of different cross-sectional dimensions joined at the plane $z = 0$. A single hybrid mode of unit amplitude

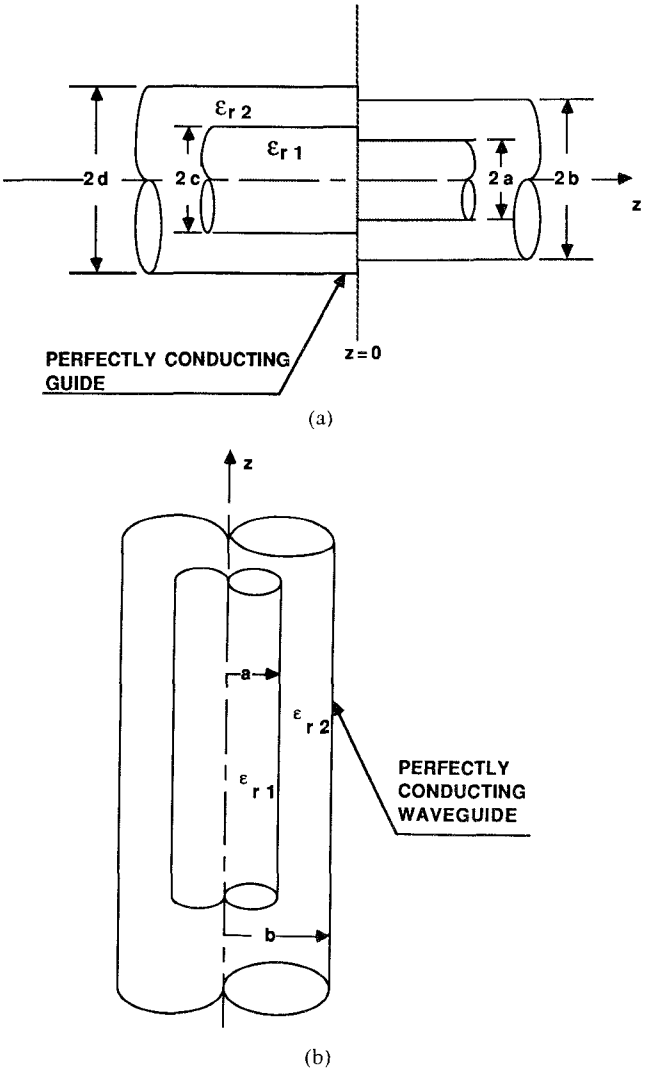

Fig. 1. Step discontinuity at the junction between two semi-infinite dielectric-loaded waveguides. (b) Dielectric-loaded waveguide

(HE_{nm}) is incident from $z < 0$ on the discontinuity. (The mode designation used throughout this paper is that introduced in [7]. Here HE_{nm} denotes a "hybrid" mode whose fields have ϕ variations $\sin n\phi$ and $\cos n\phi$ and whose propagation constants are the mth root of the characteristic equation. This designation should not be confused with "hybrid magnetic" HE and the "hybrid electric" EH des-

Manuscript received April 19, 1988; revised August 1, 1988. This work was supported by the National Science Foundation under Grant ECS-8617534.

The authors are with the Electrical Engineering Department, University of Maryland, College Park, MD 20742.

IEEE Log Number 8823767.

ignation.) It is desired to determine the amplitudes of all the reflected and transmitted hybrid modes. In particular, if complex modes can exist in either or both waveguides and these complex modes are included or excluded from the solution, what are the difference in the resulting scattering matrices?

Structures of this type can be encountered in applications in the millimeter-wave and optical frequency bands, such as in periodic structures for filtering, traveling wave tubes, backward wave oscillators, antennas and radiating elements, branching couplers for optical fibers, and millimeter-wave dielectric-loaded waveguides. The method of analysis and the results provide an accurate circuit model for the characterization of the step discontinuity in a dielectric waveguide for any hybrid mode excitation.

Before presenting the solution using mode matching, the properties of complex modes on cylindrical dielectric-loaded waveguides are summerized and typical numerical data on these modes are presented.

II. Complex Modes on Dielectric-Loaded Waveguides

Consider the infinite dielectric-loaded circular cylindrical waveguide shown in Fig. 1(b). Suppressing the axial propagation factor $e^{-\gamma z}$ and time variation factor $e^{j\omega t}$, the electromagnetic field components of the hybrid HE_{nm} modes in the guide are given by [7]

$$E_z = AR_n(\xi_i r)\cos n\phi \tag{1a}$$

$$j\omega\mu H_z = \alpha\gamma A P_n(\xi_i r)\sin n\phi \tag{1b}$$

$$\begin{bmatrix} E_r \\ \dfrac{j\omega\mu}{\gamma}H_\phi \end{bmatrix} = -\frac{A\cos n\phi}{\xi_i}\begin{bmatrix} \alpha n & 1 \\ \alpha n & -k_i^2/\gamma^2 \end{bmatrix}\begin{bmatrix} P_n(\xi_i r)/\xi_i r \\ R_n'(\xi_i r) \end{bmatrix} \tag{1c}$$

$$\begin{bmatrix} E_\phi \\ \dfrac{j\omega\mu}{\gamma}H_r \end{bmatrix} = \frac{-A\gamma\sin n\phi}{\xi_i}\begin{bmatrix} n & \alpha \\ nk_i^2 r/\gamma^2 & -\alpha \end{bmatrix} \times \begin{bmatrix} R_n(\xi_i r)/\xi_i r \\ P_n'(\xi_i r) \end{bmatrix} \tag{1d}$$

where $i=1$ for $0 \leqslant r \leqslant a$ and $i=2$ for $a \leqslant r \leqslant b$, A is an arbitrary constant, and

$$\xi_1^2 = k_1^2 + \gamma^2 \qquad \xi_2^2 = -\left(k_2^2 + \gamma^2\right) \tag{2a}$$

$$k_1^2 = \epsilon_{r_1} k_0^2 \qquad k_2^2 = \epsilon_{r_2} k_0^2 \qquad k_0^2 = \omega^2\mu_0\epsilon_0 \tag{2b}$$

$$P_n(\xi_1 r) = J_n(\xi_1 r), \qquad 0 \leqslant r \leqslant a \tag{3a}$$

$$P_n(\xi_2 r) = J_n(\xi_1 a)\left[\frac{K_n(\xi_2 r)I_n'(\xi_2 b) - I_n(\xi_2 r)K_n'(\xi_2 b)}{K_n(\xi_2 a)I_n'(\xi_2 b) - I_n(\xi_2 a)K_n'(\xi_2 b)}\right], \qquad a \leqslant r \leqslant b \tag{3b}$$

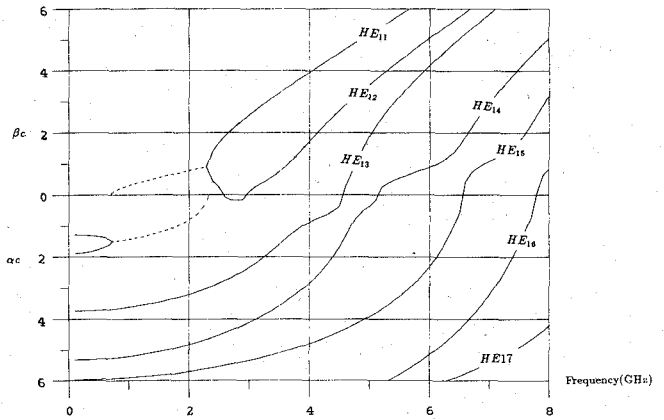

Fig. 2. $(\omega-\beta)$ diagram for the region $z<0$. $c=0.35$ in., $d=0.5$ in., $\epsilon_{r_1}=37$, $\epsilon_{r_2}=1$.

$$R_n(\xi_1 r) = J_n(\xi_1 r), \qquad 0 \leqslant r \leqslant a \tag{4a}$$

$$R_n(\xi_2 r) = J_n(\xi_1 a)\left[\frac{K_n(\xi_2 r)I_n(\xi_2 b) - I_n(\xi_2 r)K_n(\xi_2 b)}{K_n(\xi_2 a)I_n(\xi_2 b) - I_n(\xi_2 a)K_n(\xi_2 b)}\right], \qquad a \leqslant r \leqslant b \tag{4b}$$

$$\alpha = -\frac{U_n}{V_n} \tag{5}$$

$$U_n = n\gamma a J_n(\xi_1 a)\left[\frac{1}{\xi_1^2 a^2} + \frac{1}{\xi_2^2 a^2}\right] \tag{6a}$$

$$V_n = \left[\frac{J_n'(\xi_1 a)}{\xi_1 a} + \frac{P_n'(\xi_2 a)}{\xi_2 a}\right]. \tag{6b}$$

In (3) through (6), $J_n(\cdot)$, $I_n(\cdot)$, and $K_n(\cdot)$ are the Bessel functions and the modified Bessel functions of the first and second kinds, respectively.

The characteristic equation for the propagation constant γ is

$$U_n^2 + k_0^2 a^2 V_n W_n = 0 \tag{7}$$

where

$$W_n = \left[\epsilon_{r_1}\frac{J_n(\xi_1 a)}{\xi_1 a} + \epsilon_{r_2}\frac{R_n'(\xi_2 a)}{\xi_2 a}\right]. \tag{8}$$

The propagation constant γ is related to ξ_1 and ξ_2 by (2).

Complex modes are characterized by a complex propagation constant γ which is obtained by searching for complex roots of the characteristic equation (7). Since the characteristic function in (7) is a real even function of γ, its complex roots occur in conjugate pairs. Further, if γ is a root, then $(-\gamma)$ is also a root. It therefore results that there is always a quadruple of complex roots: $\pm\gamma$ and $\pm\gamma^*$. In an infinite guide with no sources at infinity, a combination of a pair of complex conjugate modes must always be present. This pair will carry only reactive power, no net real average power. Typical $(\omega-\beta)$ diagrams for two dielectric-loaded waveguides with parameters that allow complex modes to be present are shown in Figs. 2 and 3. In these figures, the propagation constants $\gamma=\alpha+j\beta$ of

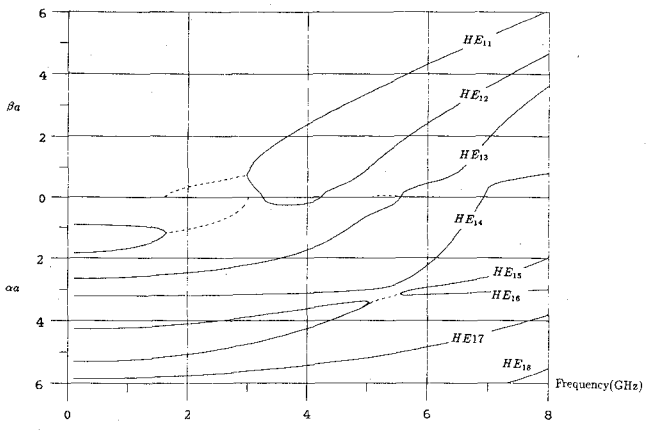

Fig. 3. $(\omega-\beta)$ diagram for the region $z>0$. $a=0.25$ in., $b=0.5$ in., $\epsilon_{r_1}=37$, $\epsilon_{r_2}=1$.

the hybrid modes with angular variation $e^{j\phi}$ in the dielectric-loaded waveguide are plotted versus frequency. The solid curve is either the purely real attenuation constant (αa) or the purely imaginary propagation constant (βa). The dotted curves are the complex propagation constant γa. Complex propagation in Fig. 3 occurs in the frequency ranges 1.7 GHz $\leqslant f \leqslant$ 3.01 GHz and 5.22 GHz $\leqslant f \leqslant$ 5.64 GHz for the hybrid modes (HE_{11}, HE_{12}) and (HE_{15}, HE_{16}), respectively. It has been shown [4] that the complex modes are linearly independent of all other propagating and evanescent modes occurring at the same frequency. Therefore expansion of any arbitrary field over the cross section of the dielectric-loaded waveguide at any frequency requires the inclusion of all complex modes that may exist. Hybrid modes, including complex modes, are complete and orthogonal over the cross sections of the guide. The orthogonality is expressed by the inner product:

$$\langle \hat{e}_j, \hat{h}_k \rangle = \int_s \left(\hat{e}_j \times \hat{h}_k\right)\cdot \hat{n}\, ds = \langle \hat{e}_j, \hat{h}_j \rangle \delta_{jk} \tag{9}$$

where j and k stand for hybrid modes HE_{mn} and $HE_{m'n'}$ with

$$\delta_{jk} = 0 \quad \text{for } j \neq k$$
$$= 1 \quad \text{for } j = k$$

and $\hat{e}_j, \hat{h}_k$ are the transverse electric and magnetic fields of the HE_{mn} and $HE_{m'n'}$ modes whose components E_r, E_ϕ, H_r, and H_ϕ are given by (1c) and (1d). Closed-form expressions for the inner products (9) are given in the Appendix.

The above properties are used in the following section to obtain a model for the step discontinuities of the dielectric-loaded waveguide shown in Fig. 1(a) using the mode-matching technique.

III. Discontinuity Characterization

Consider a hybrid HE_{mn} mode incident from $z<0$ on the step discontinuity of the two semi-infinite dielectric-loaded waveguides shown in Fig. 1(a). Due to the presence of this discontinuity, reflected and transmitted fields will be generated in the regions $z<0$ and $z>0$, respectively. Due to the uniformity of the structure in ϕ, all the fields will have the same azimuthal variation ($e^{jm\phi}$) as the incident hybrid mode. In order to calculate the reflected and transmitted fields the total transverse fields are expanded in terms of the appropriate hybrid waveguide modes on both sides of the discontinuity. Thus:

for $z<0$:

$$\overline{E}_t = \hat{e}_{A1} e^{-\gamma_{A1} z} + \sum_j A_j \hat{e}_{Aj} e^{\gamma_{Aj} z} \tag{10a}$$

$$\overline{H}_t = \hat{h}_{A1} e^{-\gamma_{A1} z} - \sum_j A_j \hat{h}_{Aj} e^{\gamma_{Aj} z} \tag{10b}$$

for $z>0$:

$$\overline{E}_t = \sum_k B_k \hat{e}_{Bk} e^{-\gamma_{Bk} z} \tag{11a}$$

$$\overline{H}_t = \sum_k B_k \hat{h}_{Bk} e^{-\gamma_{Bk} z}. \tag{11b}$$

Here $\hat{e}_{Aj}$, $\hat{h}_{Aj}$, γ_{Aj}, $\hat{e}_{Bk}$, $\hat{h}_{Bk}$, and γ_{Bk} are the transverse electric and magnetic fields and the propagation constants of the hybrid modes in the regions $z<0$ and $z>0$, respectively. Enforcing the boundary conditions requiring that the tangential electric and magnetic fields be continuous at $z=0$ then gives

$$\hat{e}_{A1} + \sum_j A_j \hat{e}_{Aj} = \sum_k B_k \hat{e}_{Bk} \tag{12a}$$

$$\hat{h}_{A1} - \sum_j A_j \hat{h}_{Aj} = \sum_k B_k \hat{h}_{Bk}. \tag{12b}$$

Taking the inner product of (12a) with $\hat{h}_{A_i}$ and $\hat{e}_{A_i}$ with (12b) and using the orthogonality relations (9), the following infinite systems of equations in the unknown coefficients A_i and B_k are obtained.

$$\sum_k X_{ik} B_k = 2\langle \hat{e}_{A_1}, \hat{h}_{A_1} \rangle \delta_{i1} \tag{13a}$$

$$\sum_k Y_{ik} B_k = 2 A_i \langle \hat{e}_{A_i}, \hat{h}_{A_i} \rangle \tag{13b}$$

where

$$X_{ik} = \langle \hat{e}_{B_k}, \hat{h}_{A_i} \rangle + \langle \hat{e}_{A_k}, \hat{h}_{B_k} \rangle \tag{14a}$$

$$Y_{ik} = \langle \hat{e}_{B_k}, \hat{h}_{A_i} \rangle - \langle \hat{e}_{A_k}, \hat{h}_{B_k} \rangle. \tag{14b}$$

The numerical solution of the system (13a) for the unknowns B_k is achieved by truncating the infinite matrix and solving the resulting finite system of linear equations. Then the A_i's are obtained using (13b).

If the modes included in (10) and (11) form a complete set (which must include any complex modes), then the solution for the reflected and transmitted field coefficients will always converge to the correct answer. If the complex modes are not included the solution may not converge or may converge to the wrong answer.

IV. Numerical Results

This section presents numerical examples illustrating the above analysis. The $(\omega-\beta)$ diagrams for the two semi-infinite waveguides in the region $z<0$ and $z>0$ are

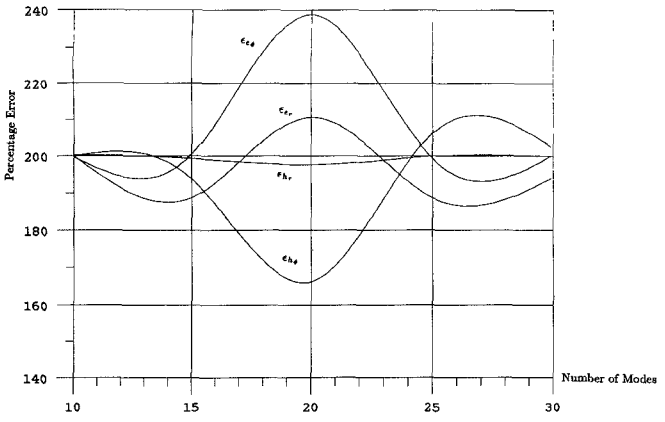

Fig. 4. Variation of the percentage error in field intensity with number of modes without including complex modes.

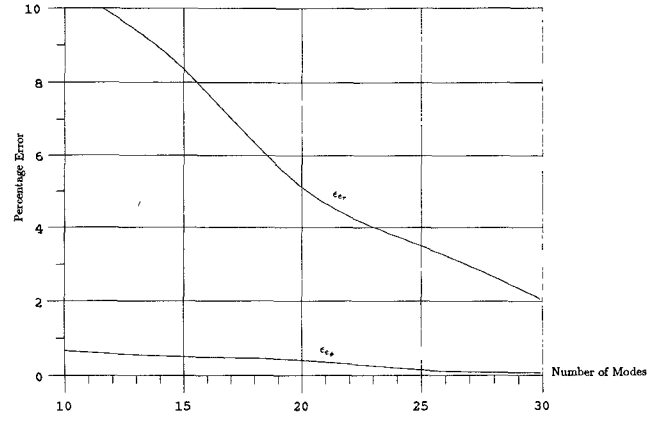

(a)

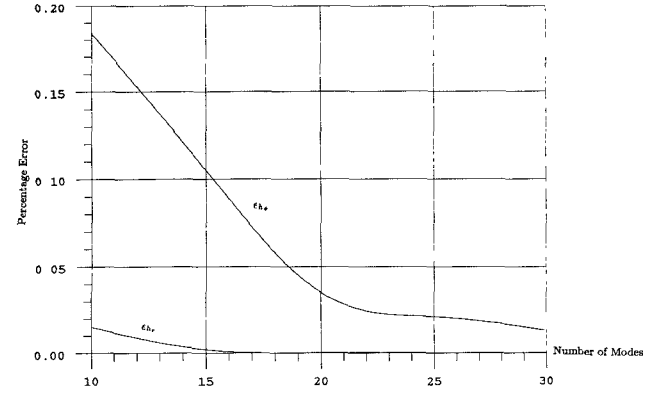

(b)

Fig. 5. (a) Variation of the percentage error in field intensity with number of modes when complex modes are included. (b) Variation of the percentage error in field intensity with number of modes when complex modes are included.

shown in Figs. 2 and 3, respectively. The field solutions due to the discontinuity are obtained with and without the inclusion of the complex modes. To check the validity of the solution, the total fields were computed from the coefficients of expansion, and the boundary conditions which these fields must satisfy at $z = 0$ are verified. A quantitative measure of the error in satisfying the boundary conditions in the electric and magnetic field components used in the computation is defined by

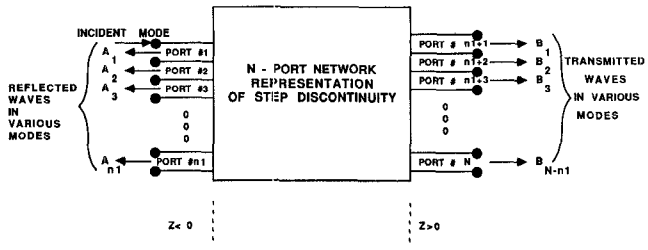

Fig. 6. Network representation of the step discontinuity.

$$\epsilon = 4\frac{\int_S |(\text{field component at } z = 0^+) - (\text{field comoponent at } z = 0^-)|^2\, dS}{\int_S |(\text{field component at } z = 0^+) + (\text{field component at } z = 0^-)|^2\, dS} \tag{15}$$

where S is the guide cross section. It was found that when the complex modes are not included, the boundary conditions at $z = 0$ are not satisfied, regardless of the number of modes included in the solution, as shown in Fig. 4. On the other hand, when the complex modes are included in the expansion, the boundary conditions are satisfied and the error in the boundary conditions decreases monotonically as the number of modes is increased, as shown in Fig. 5(a) and (b).

The complete scattering matrix which completely characterizes the step discontinuity is easily obtainable from the results of the above analysis. A circuit representation of the junction discontinuity is shown in Fig. 6. This representation is an N-port network, with ports $1, 2, \cdots, n_1$ corresponding to the modes in the dielectric-loaded waveguide in the region $z < 0$, while the ports n_1+1, $n_1+2, \cdots, N$ correspond to the modes in the waveguide region $z > 0$. The expansion coefficients A_i and B_k in (10) and (11) can be taken as proportional to incident and scattered waves on the multiport network. The proportionality constants are the normalization factors $\langle \hat{e}_{A_i}, \hat{h}_{A_i} \rangle$ or $\langle \hat{e}_{B_k}, \hat{h}_{B_k} \rangle$, respectively. Thus, when a unit incident wave of the mode corresponding to port 1 is incident on port 1, the elements of one row of the scattering matrix are computed as

$$s_{j1} = A_j \frac{\langle \hat{e}_{A_1}, \hat{h}_{A_1} \rangle}{\langle \hat{e}_{A_j}, \hat{h}_{A_j} \rangle}, \qquad j = 1, 2, \cdots, n_1$$

$$= B_{j-n_1} \frac{\langle \hat{e}_{A_1}, \hat{h}_{A_1} \rangle}{\langle \hat{e}_{B_{j-n_1}}, \hat{h}_{B_{j-n_1}} \rangle}, \qquad j = n_1+1, \cdots, N.$$

Other elements of the scattering matrix are similarly defined. Scattering parameters for several cases in various frequency bands were computed. Fig. 7 shows the variation with frequency of the scattering matrix coefficients for a step discontinuity in a dielectric-loaded waveguide, with $\epsilon_r = 71$. The parameters allow only one propagating mode in the guide region $z < 0$, and two modes in the region $z > 0$. A complex mode exists in the band of frequencies shown. The 3×3 scattering matrix elements shown in Fig. 7 correspond to the three propagating modes.

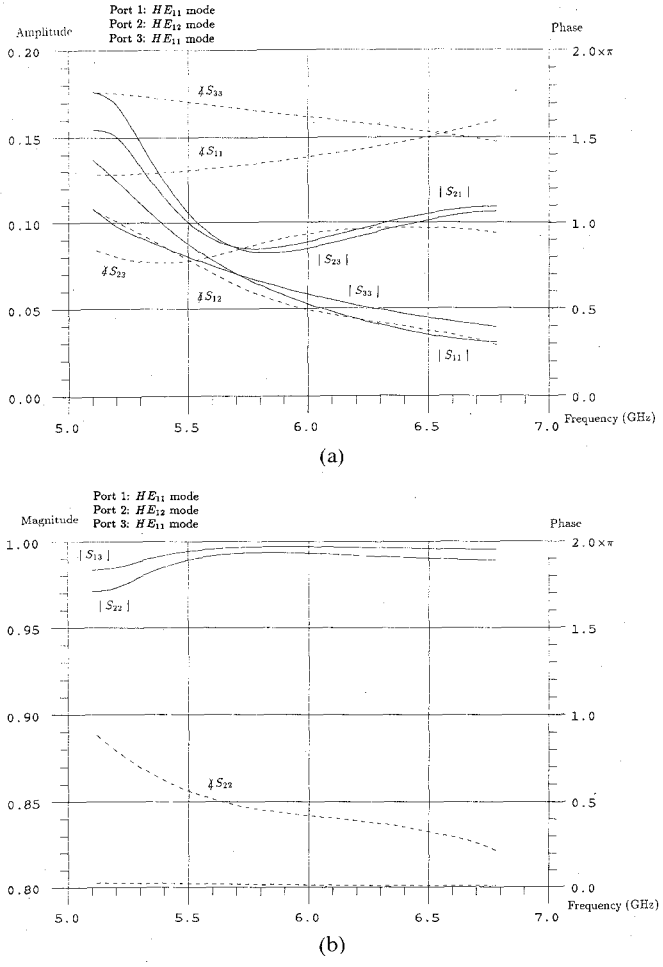

Fig. 7. (a) Frequency variation of the scattering matrix elements ($S_{11}, S_{21}, S_{23}, S_{33}$) of a step discontinuity. $a = 0.120$ in., $b = 0.216$ in., $c = 0.16$ in., $d = 0.216$ in., $\epsilon_{r_1} = 71$, $\epsilon_{r_2} = 1$. (b) Frequency variation of the scattering matrix elements of (S_{13} and S_{22}) of a dielectric step discontinuity. $a = 0.120$ in., $b = 0.216$ in., $c = 0.16$ in., $d = 0.216$ in., $\epsilon_{r_1} = 71$, $\epsilon_{r_2} = 1$.

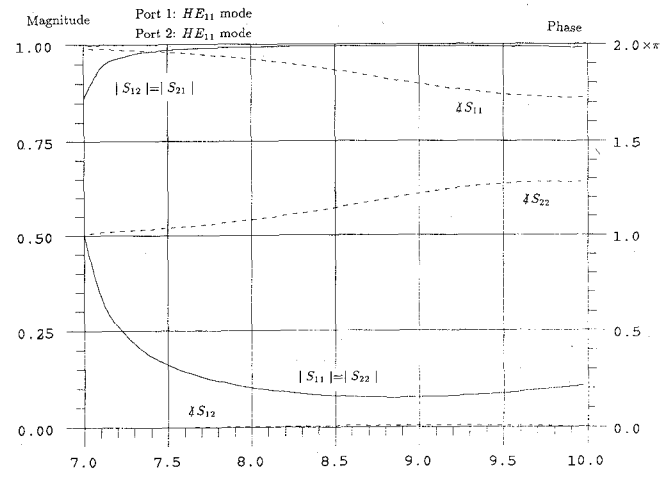

Fig. 8. Frequency variation of the scattering matrix elements of a step discontinuity in an X-band dielectric-loaded waveguide. $a = 0.120$ in., $b = 0.45$ in., $c = 0.16$ in., $d = 0.45$ in., $\epsilon_{r_1} = 6.6$, $\epsilon_{r_2} = 1$.

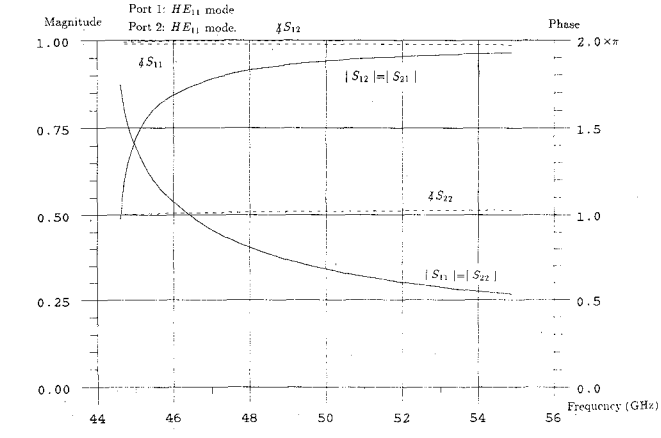

Fig. 9. Frequency variation of the scattering matrix elements of a step discontinuity in a millimeter-wave dielectric-loaded waveguide. $a = 0.015$ in., $b = 0.075$ in., $c = 0.05$ in., $d = 0.075$ in., $\epsilon_{r_1} = 2.55$, $\epsilon_{r_2} = 1$.

Figs. 8 and 9 show the variation with frequency of the 2×2 scattering matrix elements for a step discontinuity in the dielectric-loaded waveguides in the X-band (7–10 GHz) and millimeter-wave band (44–56 GHz), respectively.

V. Conclusion

It is shown through numerical calculations of specific examples that complex modes are part of a complete set that represent the total fields in dielectric-loaded waveguides. Solution of the step discontinuity problem in a dielectric-loaded waveguide has been obtained using mode matching, and verification of the accuracy and convergence of the solution has been presented. A circuit model for the step discontinuity in a hybrid mode dielectric-loaded waveguide is given in terms of the scattering matrix of a multiport network.

Examples are presented in the microwave (C and X) bands for the HE_{11} mode, as well as in the millimeter-wave range. This type of transmission medium is useful for millimeter, submillimeter, and optical wavelengths. In order to reduce the transmission loss, higher order modes may be used. The technique presented for the discontinuity characterization is general and applicable for any mode and frequency band.

Appendix
Analytic Expressions for the Inner Products of (9)

This Appendix gives analytic expressions of the inner products defined in (9). The two waveguides have the same outside conductor radius ($c = d$) but different dielectric radii ($a \neq b$). The field quantities in the two waveguides are denoted by the suffixes i and j, respectively.

$$\langle E_{\mathrm{HE}_i}, H_{\mathrm{HE}_j} \rangle = -\gamma_{\mathrm{HE}_i} \Big\{ \Big[\Big(k_3^2 - \alpha_i \alpha_j \gamma_{\mathrm{HE}_j}^2 \Big) F + \Big(\alpha_i k_3^2 - \alpha_j \gamma_{\mathrm{HE}_j}^2 \Big) G \Big] + \Big[-\alpha_i \alpha_j \gamma_{\mathrm{HE}_j}^2 H + k_4^2 I - \alpha_j \gamma_{\mathrm{HE}_j}^2 J + \alpha_i k_2^2 K \Big] + \Big[k_4^2 M - \alpha_i \alpha_j \gamma_{\mathrm{HE}_j}^2 L + \alpha_i k_4^2 N - \alpha_j \gamma_{\mathrm{HE}_j}^2 O \Big] \Big\}$$

$$\langle E_{\mathrm{HE}_j}, H_{\mathrm{HE}_i}\rangle = \gamma_{\mathrm{HE}_j}\Big\{\Big[\big(k_1^2-\alpha_i\alpha_j\gamma_{\mathrm{HE}_i}^2\big)F + \big(\alpha_j k_1^2-\alpha_i\gamma_{\mathrm{HE}_i}^2\big)G\Big] - \Big[k_1^2 I+\alpha_j k_1^2 J-\alpha_i\gamma_{\mathrm{HE}_i}^2 K-\alpha_i\alpha_j\gamma_{\mathrm{HE}_i}^2 H\Big] - \Big[k_2^2 L+\alpha_j k_2^2 O-\alpha_i\gamma_{\mathrm{HE}_i}^2 N-\alpha_i\alpha_j\gamma_{\mathrm{HE}_i}^2 M\Big]\Big\}$$

$$\langle E_{\mathrm{TE}_i}, H_{\mathrm{TE}_j}\rangle = \gamma_{\mathrm{TE}_j}[F-H-L]$$

$$\langle E_{\mathrm{TE}_j}, H_{\mathrm{TE}_i}\rangle = \gamma_{\mathrm{TE}_i}[F-H-L]$$

$$\langle E_{\mathrm{TM}_i}, H_{\mathrm{TM}_j}\rangle = -\gamma_{\mathrm{TM}_i}\big[k_3^2F-k_4^2I-k_4^2M\big]$$

$$\langle E_{\mathrm{TM}_j}, H_{\mathrm{TM}_i}\rangle = -\gamma_{\mathrm{TM}_j}\big[k_1^2F-k_1^2I-k_2^2M\big]$$

$$\langle E_{\mathrm{HE}_i}, H_{\mathrm{HE}_i}\rangle = -\gamma_{\mathrm{HE}_i}\Big\{\Big[\big(k_1^2-\gamma_{\mathrm{HE}_i}^2\alpha_i^2\big)Q + \big(k_1^2-\gamma_{\mathrm{HE}_i}^2\big)\alpha_i S\Big] - k_2^2T+\gamma_{\mathrm{HE}_i}^2\alpha_i^2U+\alpha_i\big(\gamma_{\mathrm{HE}_i}^2-k_2^2\big)V\Big\}$$

$$\langle E_{\mathrm{TE}_i}, H_{\mathrm{TE}_i}\rangle = \gamma_{\mathrm{TE}_i}\{Q+U\}$$

$$\langle E_{\mathrm{TM}_i}, H_{\mathrm{TM}_i}\rangle = -\gamma_{\mathrm{TM}_i}\{k_1^2Q+k_2^2T\}$$

where

$$F=\frac{1}{\xi_i^2\xi_j^2}\left[\frac{\xi_i^2\xi_j a}{\xi_i^2-\xi_j^2}J_n(\xi_i a)J_n'(\xi_j a)+\frac{\xi_j^2\xi_i a}{\xi_j^2-\xi_i^2}J_n'(\xi_i a)J_n(\xi_j a)\right]$$

$$G=\frac{n}{\xi_i^2\xi_j^2}J_n(\xi_i a)J_n(\xi_j a)$$

$$H=\frac{1}{\xi_i^2\zeta_j^2}\left[\frac{\xi_i^2\zeta_j r}{\xi_i^2+\zeta_j^2}J_n(\xi_i r)P_n'(\zeta_j r)+\frac{\zeta_j^2\xi_i r}{\zeta_j^2+\xi_i^2}J_n'(\xi_i r)P_n(\zeta_j r)\right]\Bigg|_a^b$$

$$I=\frac{1}{\xi_i^2\zeta_j^2}\left[\frac{\xi_i^2\zeta_j r}{\xi_i^2+\zeta_j^2}J_n(\xi_i r)R_n'(\zeta_j r)+\frac{\zeta_j^2\xi_i r}{\zeta_j^2+\xi_i^2}J_n'(\xi_i r)R_n(\zeta_j r)\right]\Bigg|_a^b$$

$$J=\frac{n}{\xi_i^2\zeta_j^2}J_n(\xi_i r)P_n(\zeta_j r)\Bigg|_a^b$$

$$K=\frac{n}{\xi_i^2\zeta_j^2}J_n(\xi_i r)R_n(\zeta_j r)\Bigg|_a^b$$

$$L=\frac{1}{\zeta_i^2\zeta_j^2}\left[\frac{\zeta_i^2\zeta_j b}{\zeta_i^2-\zeta_j^2}J_n(\xi_i b)P_n(\zeta_j b)+\frac{\zeta_j^2\zeta_i b}{\zeta_j^2-\zeta_i^2}P_n(\zeta_i b)P_n(\zeta_j b)\right]$$

$$M=\frac{1}{\zeta_i^2\zeta_j^2}\left[\frac{\zeta_i^2\zeta_j b}{\zeta_i^2-\zeta_j^2}J_n(\xi_i b)R_n(\zeta_j b)+\frac{\zeta_j^2\zeta_i b}{\zeta_j^2-\zeta_i^2}R_n(\zeta_i b)R_n(\zeta_j b)\right]$$

$$N=\frac{n}{\zeta_i^2\zeta_j^2}J_n(\xi_i b)R_n(\zeta_j b)$$

$$O=\frac{n}{\zeta_i^2\zeta_j^2}J_n(\xi_i b)P_n(\zeta_j b)$$

$$Q=\frac{b^2}{2\xi_i}\left[\left(1-\frac{n^2}{\xi_i^2b^2}\right)J_n^2(\xi_i b)+J_n'^2(\xi_i r)+\frac{2}{\xi_i b}J_n(\xi_i b)J_n'(\xi_i b)\right]$$

$$S=\frac{n}{\xi_i^4}J_n^2(\xi_i b)$$

$$T=\frac{r^2}{2\zeta_i^2}\left[\left(1+\frac{n^2}{\zeta_i^2r^2}\right)R_n^2(\zeta_i r)-R_n'^2(\zeta_i r)-\frac{2}{\zeta_i r}R_n(\zeta_i r)R_n'(\zeta_i r)\right]\Bigg|_b^c$$

$$U=\frac{r^2}{2\zeta_i^2}\left[\left(1+\frac{n^2}{\zeta_i^2r^2}\right)P_n^2(\zeta_i r)-P_n'^2(\zeta_i r)-\frac{2}{\zeta_i r}P_n(\zeta_i r)P_n'(\zeta_i r)\right]\Bigg|_b^c$$

$$V=\frac{n}{\zeta_i^4}J_n^2(\xi_i b).$$

Note that in the above equations,

$$\xi_i^2=k_1^2+\gamma_i^2 \qquad \zeta_i^2=-\big(k_2^2+\gamma_i^2\big)$$

$$\xi_j^2=k_1^2+\gamma_j^2 \qquad \zeta_j^2=-\big(k_2^2+\gamma_j^2\big).$$

REFERENCES

[1] P. J. B. Clarricoates and B. C Taylor, "Evanescent and propagating modes of dielectric loaded circular waveguide," *Proc. Inst. Elec. Eng.*, vol. 111, pp. 1951-1956, dec. 1964.

[2] T. Tamir and A. A. Oliner, "Guided complex modes," *Proc. Inst. Elec. Eng.*, vol. 110, no. 2, pp. 310–324, Feb. 1963.

[3] S. B. Rayevskiy, "Some properties of complex waves in a double layer, circular, shielded waveguide," *Radio Eng. Electron. Phys.*, vol. 21, pp. 36–39, 1976.

[4] A. S. Omar and K. F. Schunemann, "Complex and backward-wave modes in inhomogeneously and anisotropically filled waveguides," *IEEE Trans. Microwave Theory Tech.*, vol. MTT-35, pp. 268–275, Mar. 1987.

[5] K. A. Zaki and C. Chen, "Complex modes in dielectric loaded waveguides," in *IEEE AP-S Int. Symp. Dig.*, June 1987, pp. 8–11.

[6] A. S. Omar and K. F. Schunemann, "The effect of complex modes at finline discontinuities," *IEEE Trans. Microwave Theory Tech.*, vol. MTT-34, pp. 1508–1514, Dec. 1986.

[7] K. A. Zaki and A. E. Atia, "Modes in dielectric loaded waveguides and resonators," *IEEE Trans. Microwave Theory Tech.*, vol. MTT-31, pp. 1039–1045, Dec. 1983.

✠

Kawthar A. Zaki (SM'85) received the B.S. degree (with honors) from Ain Shams University, Cairo, Egypt, in 1962 and the M.S. and Ph.D. degrees from the University of California, Berkeley, in 1966 and 1969, respectively, all in electrical engineering.

From 1962 to 1964, she was a Lecturer in the Department of Electrical Engineering, Ain Shams University. From 1965 to 1969, she held the position of Research Assistant in the Electronic Research Laboratory, University of California, Berkeley. She joined the Electrical Engineering Department, University of Maryland, College Park, in 1970, where she is presently Professor of Electrical Engineering. Her research interests are in the areas of electromagnetics, microwave circuits, optimization, computer-aided design, and optically controlled microwave and millimeter-wave devices.

Dr. Zaki is a member of Tau Beta Pi.

Seng-Woon Chen (S'87) was born in Keelung, Taiwan, in 1961. He received the B.S. degree in electrical engineering from National Taiwan University in 1982.

During the years 1982–1984, he was with the China Military Police Headquarters as a member of the technical staff. Beginning in 1984, he spent two years as a member of the technical staff at Microelectronics Technology Inc, Taiwan, where his research dealt mainly with *K*-band MESFET dielectric resonator oscillators, voltage-controlled oscillators, and phase-locked oscillators. Since 1986, he has been a graduate student in the Electrical Engineering Department, University of Maryland at College Park, where he is working toward the Ph.D degree under the supervision of Dr. K. A. Zaki. His research interests are the modeling of microwave and millimeter-wave circuits.

✠

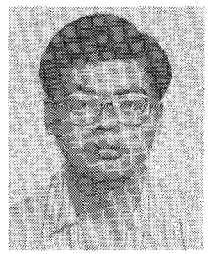

Chunming Chen (S'85) was born in Taiwan, Republic of China, in 1958. He received the B.S. degree from the National Tsing Hua University, Taiwan, in 1981 and the M.S. degree from the University of Maryland, College Park, in 1985, both in electrical engineering. Since 1984, he has worked as a research assistant in Department of Electrical Engineering, University of Maryland, College Park. He is now working towards the Ph.D. degree in the area of microwave components and circuits.